Z. Phys. C – Particles and Fields 12, 297–306 (1982)

Zeitschrift für Physik C Particles and Fields

Energy Dependence of Jet Measures in e^+e^- Annihilation

Pluto Collaboration

Ch. Berger, H. Genzel, R. Grigull, W. Lackas, F. Raupach, W. Wagner
I. Physikalisches Institut der RWTH Aachen[1], D-5100 Aachen, Federal Republic of Germany

A. Klovning, E. Lillestöl
University of Bergen[2], N-5000 Bergen, Norway

H. Ackermann, G. Alexander[3], G. Bella[3], J. Bürger, L. Criegee, A. Eskreys[4], G. Franke, Ch. Gerke, G. Knies, E. Lehmann, U. Michelsen, K. H. Pape, H. D. Reich, J. M. Scarr[5], B. Stella[6], U. Timm, G. G. Winter, S. T. Xue[7], W. Zimmermann
Deutsches Elektronen-Synchrotron DESY, D-2000 Hamburg, Federal Republic of Germany

O. Achterberg, V. Blobel, L. Boesten, V. Hepp[8], H. Kapitza, B. Koppitz, B. Lewendel, W. Lührsen, R. van Staa, H. Spitzer
II. Institut für Experimentalphysik der Universität, D-2000 Hamburg[1], Federal Republic of Germany

C. Y. Chang, R. G. Glasser, R. G. Kellogg, K. H. Lau, R. O. Polvado, B. Sechi-Zorn, J. A. Skard, A. Skuja, G. Welch, G. T. Zorn
University of Maryland[9], College Park, MD 20742, USA

A. Bäcker, F. Barreiro, S. Brandt, K. Derikum, C. Grupen, H. J. Meyer, B. Neumann, M. Rost, K. Stupperich, G. Zech
Universität-Gesamthochschule, D-5900 Siegen[1], Federal Republic of Germany

H. J. Daum, H. Meyer, O. Meyer, D. Schmidt
Universität-Gesamthochschule, D-5600 Wuppertal[1], Federal Republic of Germany

Received 22 December 1981

Abstract. The jet character of the hadronic final states produced in e^+e^- annihilations is studied in terms of jet measures such as thrust, sphericity, jet opening angle and jet masses, in the energy range 7.7 to 31.6 GeV. All distributions and averages have been corrected for detector effects and initial state radiation. The energy dependence of the averages of these jet quantities is used to estimate the contributions due to perturbative QCD and fragmentation effects. Correlations between the jet measures and the multiplicity of charged hadrons are also presented.

I. Introduction

A great deal of attention has been paid to the study of jet formation in hadron-hadron, lepton-hadron and lepton-lepton interactions as a possible signature of hard parton reactions. In the case of hadronic final states produced in e^+e^- annihilation, evidence for two jet production was found at SPEAR and DORIS [1]. With the advent of the high energies available at PETRA, evidence for a departure from the two jet

1 Supported by the BMFT, FRG
2 Partially supported by the Norwegian Council for Science and Humanities
3 On leave from Tel Aviv University, Israel
4 Now at Institute of Nuclear Physics, Krakow, Poland
5 On leave from University of Glasgow, Scotland
6 Now at University of Rome, Italy; partially supported by INFN
7 On leave from Institute of High Energy Physics, Academia Sinica, Peking, The People's Republic of China
8 Now at Heidelberg University, FRG
9 Partially supported by Department of Energy, USA

0170-9739/82/0012/0297/$02.00

topology was found [2]. Our current understanding of two and three jet production in e^+e^- annihilation at high energies [3, 4] is based on QCD the dynamical theory of quarks and vector gluons. In this theory the originally produced quark-antiquark pair may radiate gluons which in turn may develop into independent jets. Thus the manifest three jet structures observed at PETRA are interpreted as due to hard gluon bremsstrahlung. Since the "bremsstrahlung" process favours low gluon energies, the number of clearly observable 3-jet events is small compared to the bulk of events in which the 3-jet structure is less obvious, or even completely masked by fragmentation effects.

In an earlier paper [4] we have isolated a sizeable fraction of all hadronic events ($\sim 15\%$) as due to gluon bremsstrahlung and exploited them for determining the quark-gluon coupling constant α_s.

In contrast, the present investigation makes no attempt to separate different topologies, but extracts from the total sample of hadronic events several jet measures such as thrust, sphericity, jet opening angle and jet masses. By studying the energy dependence of the average jet measures one can then separate the effects of the fragmentation which are expected [5] to fall like $s^{-1/2}$ from those of gluon radiation which vary only logarithmically with the energy. This simple parametrization allows a consistent description of the energy dependence of all these jet measures, with values of α_s which are close to the ones obtained via more involved Monte Carlo simulations of the fragmentation process [3, 4].

A special effort has been made to unfold all the distributions and averages presented from experimental biases and resolution effects, as well as from the influence of initial state photon radiation (which is also detector dependent). This allows a direct comparison with the corresponding theoretical predictions (on the hadron level, of course), as well as with corrected data from other experiments [3d].

The paper is organized as follows. In Sect. II we describe the experimental procedure. We present thrust distributions in Sect. III, and sphericity distributions in Sect. IV. In Sect. V we study the energy dependence of the jet opening angle while Sect. VI is devoted to a study of jet masses. The energy dependence of $\langle n_{\mathrm{ch}} \rangle$, the mean charged multiplicity, on c.m. energy and on each of the previously mentioned jet measures is described in Sect. VII. Finally Sect. VIII contains a summary and conclusions.

II. Experimental Setup

The data presented in this paper have been obtained with the PLUTO detector operating at DORIS and PETRA, the e^+e^- storage rings at DESY, Hamburg. Details on the detector have been published elsewhere [6]. Here it suffices to say that PLUTO is a magnetic detector with a tracking device consisting of thirteen layers of cylindrical proportional wire chambers providing charged particle recognition over 87% of 4π. Barrel (8.6 radiation lengths) and endcap (10.5 radiation lengths) lead scintillator shower counters cover 96% of the full solid angle and are used for detection of neutral particles. The data used in the present study were taken at center of mass energies of 7.7*, 9.4, 12, 13, 17, 22, 27.6 GeV and in an energy scan between 30.0 and 31.6 GeV [7]. The data selection criteria are similar to those already described in [4]. They amount basically to demanding that

a) the visible energy is greater than half of the nominal c.m. energy,

b) at least four charged tracks must belong to a common vertex,

c) the reconstructed interaction vertex lies within ± 4 cm of the center of the bunch-bunch collision, and

d) the angle of the jet axis with respect to the beam, θ, satisfies the condition $|\cos\theta| < 0.75$.

Events satisfying these criteria were visually scanned in order to reject contamination from higher order QED processes and cosmic showers. The accepted sample thus contains a negligible amount of background events. For the purpose of reconstructing the hadronic energy the pion mass was assigned to charged particles and the photon mass to neutral ones. Details on the reconstruction of neutral particles from the shower counter information are given in [8].

III. Thrust Distributions

Thrust [9] is calculated as

$$T = \max \frac{\sum_i |p_{\|_i}|}{\sum_i |\boldsymbol{p}_i|}, \tag{1}$$

where $p_{\|_i}$ is the longitudinal momentum of the i^{th} particle with respect to the jet axis and the sum runs over all particles, charged and neutrals. Physically, the values of T are restricted to the range $0.5 < T < 1$.

The thrust distributions have been corrected for a) initial state radiation, b) detector acceptance and resolution and c) track analysis and event selection criteria. We have done this by comparing the thrust distribution, the mean thrust value and the thrust axis angular distribution for Monte Carlo simulated events à la Hoyer et al. [10] before and after passing them

* For the 7.7 GeV data only charged particle information has been used in the present analysis

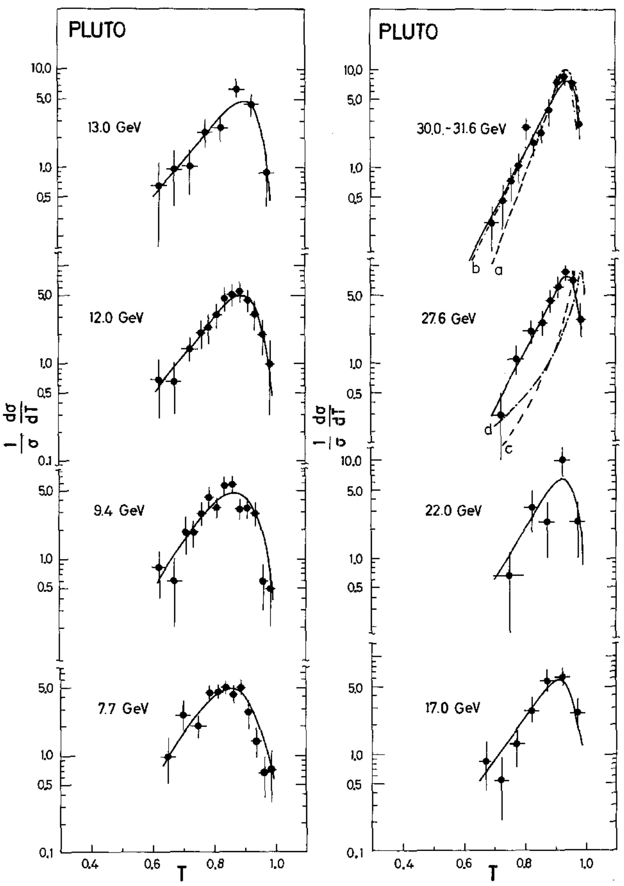

Fig. 1. Normalized thrust distributions from 7.7 up to 31.6 GeV. The solid line represents the expectations from Field and Feynman [12] and from Hoyer et al. [10] models for energies below and above 20 GeV respectively. The 30–31.6 GeV data is also compared to Monte Carlo calculations a) without gluon radiation, [12] (dashed line) and b) multiple gluon emission, [14a] (LLA) dashed-dotted line. The 27.6 GeV data is also compared to c) pure QCD predictions in first order, (2) (dashed) and d) leading (dashed-dotted) order, (15)

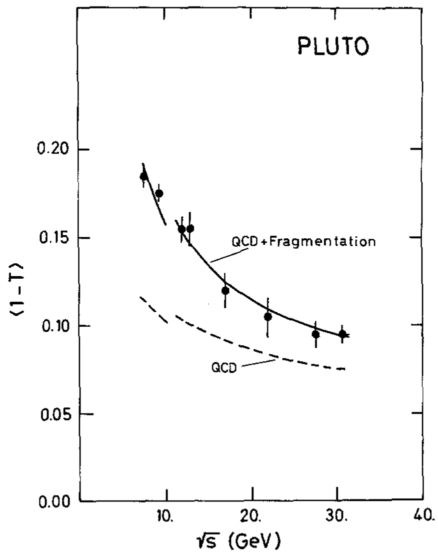

Fig. 2. Mean thrust values as a function of c.m. energy. The solid line represents the results of fitting the linear sum of a QCD perturbative term (dashed line) and a fragmentation term. The break in the curves is due to the increase in the number of flavours, (4), when crossing the $b\bar{b}$ threshold

through a complete simulation of our detector effects, selection cuts and initial state radiation. We have found that the thrust distributions for Monte Carlo events before and after detector simulation have a similar shape with mean values which are $\lesssim 5\%$ higher in the sample before detector. Furthermore the mean value for the angle between the reconstructed thrust axis after including detector simulation and the generated axis is 6° at 30 GeV. All of these results are furthermore insensitive to the exclusion of neutrals. The fully corrected data are obtained by applying to our observed thrust distribution a bin by bin correction factor which is deduced from the comparison between Monte Carlo samples before and after the detector simulation previously described. This correction is found to be typically of the order of or smaller than 10%.

In order to check the correction procedure and to estimate our systematic errors we repeated the calculations of thrust not with respect to a single axis but partitioning a given event into two disjoint classes such that the sum of the longitudinal momenta along these two axes is maximized. After corrections for initial state radiation the two methods should yield the same numerical value for thrust. For this purpose the algorithm developed in [11] has been used. The corrected results obtained are found to be in agreement within statistical errors with those previously described. We do not know of any systematic source of error which could contribute more than 5% to the mean value of $(1-T)$.

The fully corrected thrust distribution from 7.7 to 31.6 GeV is presented in Fig. 1. The general features of the data are

i) the thrust distribution is broad at low energies, but narrows with increasing energy,

ii) as the energy increases the position of the peak shifts towards high thrust values indicating a narrowing of the jets.

These features are well described by the Field and Feynman Monte Carlo model [12] at low energies and by Monte Carlo models which include QCD effects at first, second or leading – log order [10, 13, 14] at the higher energies. This is demonstrated in Fig. 1 by the full line which is calculated from [12] below 20 GeV and from [10] above. The dashed line a at the highest energy, 30.0 – 31.6 GeV, calculated from [12], indicates the necessity to include gluon emission in the Monte Carlo, the dot-dashed line b from [14a] shows however similar good agreement with the data as does the first order QCD Monte Carlo from [10].

The mean value of $(1-T)$ as presented in Fig. 2 displays a strong decrease with increasing energy, corresponding to the shift of the peak in the thrust distributions. The thrust, T, being linear in particle momenta, is considered to be infra-red stable, and its distribution has been calculated in QCD perturbation theory. The first order calculation yields [5]

$$\frac{1}{\sigma_0}\frac{d\sigma}{dT}=\frac{2\alpha_s}{3\pi}\left[\frac{6T^2-6T+4}{T(1-T)}\ln\frac{2T-1}{(1-T)}-\frac{(6T-4)(2-T)}{(1-T)}\right], \tag{2}$$

where σ_0 is the total hadronic cross-section. It can be integrated to give*

$$\langle 1-T\rangle=1.05\frac{\alpha_s}{\pi}, \tag{3}$$

where α_s is the strong coupling constant, and its dependence on energy is given to first order by

$$\alpha_s=\frac{4\pi}{(11-\frac{2}{3}N_f)\ln\frac{s}{\Lambda^2}}. \tag{4}$$

N_f being the number of flavours, s the square of the c.m. energy and Λ the QCD scale parameter.

For thrust values close to 1, multiple gluon emission becomes important and leads to a damping and a cancellation of the singularity apparent in (2) for $T\to 1$. The multiple soft gluon emission can be summed in all orders of perturbation theory using the leading logarithmic approximation (LLA) resulting in [17]

$$\frac{1}{\sigma_0}\frac{d\sigma}{dT}=\frac{8\alpha_s}{3\pi}\frac{|\ln(1-T)|}{1-T}\exp\left(-\frac{4\alpha_s}{3\pi}\ln^2(1-T)\right). \tag{5}$$

Also in this expression, the average value of $(1-T)$ exhibits no other energy dependence than that implicit in α_s resulting in a weak dependence on the energy, in contrast to the data displayed in Fig. 2. The analytical expressions (2) and (5) derived in first or leading order are too narrow to describe the data as shown in Fig. 1, by the dashed line c at 27.6 GeV for (2) and by the dot-dashed line d for (5). This difference is indicative of the presence of nonperturbative (hadronization) effects at PETRA energies.

An estimate of these non-perturbative effects is given by the expression*:

$$\langle 1-T\rangle_{\mathrm{NP}}\simeq\frac{C\langle p_T\rangle_{\mathrm{NP}}}{\sqrt{s}}, \tag{6}$$

where C is related to the total non-perturbative mean multiplicity by $\langle n\rangle = C\ln\sqrt{s}+\text{const}$ and $\langle p_T\rangle_{\mathrm{NP}}$ is the mean transverse momentum of particles in the limit of zero longitudinal momentum. For small values of $1-T$ the QCD-contribution and the non-perturbative contributions can be added linearly [5]:

$$\langle 1-T\rangle=1.05\frac{\alpha_s}{\pi}+\frac{C\langle p_T\rangle_{\mathrm{NP}}}{\sqrt{s}}. \tag{7}$$

Fitting α_s and $C\langle p_T\rangle_{\mathrm{NP}}$ to our data yields $\alpha_s=0.22\pm 0.02$ (at 30 GeV) and $C\langle p_T\rangle_{\mathrm{NP}}=0.60\pm 0.15$ GeV in reasonable agreement with what we have obtained in a study of energy-energy correlations [21]. Second order perturbation theory adds a term $C_2\cdot\left(\frac{\alpha_s}{\pi}\right)^2$ to (7). Inserting the published value [16] $C_2=9.5$ does not change the partition into QCD and non-perturbative parts, but only produced a reduction of α_s to the value 0.15 ± 0.02**. As shown in Fig. 2, solid line, the data is well described by the fit to (7).

We should also point out that none of the bare QCD predictions discussed so far can describe the energy dependence of $\langle 1-T\rangle$ for reasonable values of Λ ($\Lambda\lesssim 2$ GeV). It thus appears that the proposed splitting of the energy dependence into a logarithmic term, determined from perturbative QCD, and a non-perturbative one decreasing like $1/\sqrt{s}$, works very well in the range from 8 to 32 GeV. This indicates that the non-perturbative contribution to thrust, although dying away rapidly cannot be neglected at PETRA energies.

IV. Sphericity Distributions

Sphericity [19] is defined as

$$S=\tfrac{3}{2}\min\frac{\sum_i p_{T_i}^2}{\sum_i |\boldsymbol{p}_i|^2},$$

where p_{T_i} is the transverse momentum of the i^{th} particle with respect to the jet axis and the sum extends

* Here the average is defined as $\langle 1-T\rangle=\frac{1}{\sigma_0}\int_{T_{\min}}^{T_{\max}}\frac{d\sigma}{dT}(1-T)dT$ with $T_{\min}=2/3$ and $T_{\max}$ set to 1

* $\langle 1-T\rangle_{\mathrm{NP}}$ is derived using an independent-particle model with a longitudinal phase space of the form $d^3n=f(z,p_T)d^3p/E$ where $z=p_{\|}/E_{\mathrm{beam}}$

** As G. Kramer pointed out to us, a different treatment of the soft gluons is expected to lead to a smaller value of the second-order corrections, and therefore to a smaller change in α_s

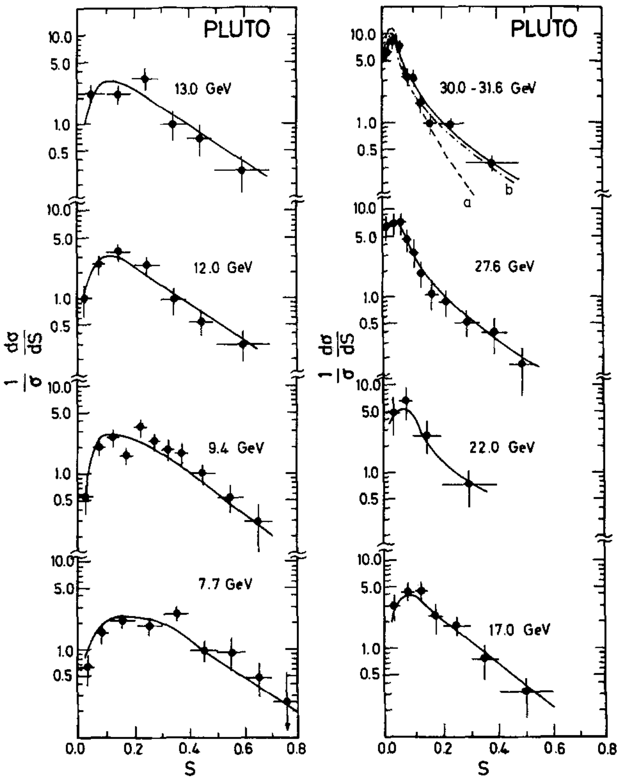

Fig. 3. Normalized sphericity distributions from 7.7 up to 31.6 GeV. The solid line represents the expectations from Monte Carlo calculations according to Field and Feynman (for energies below 20 GeV) and Hoyer et al. (above). The 30.0–31.6 GeV data is also compared to Monte Carlo calculations a) without gluon radiation (dashed line) and b) multiple gluon emission in the LLA (dashed-dotted line)

over all particles. Since sphericity is quadratic in the momenta* it cannot be calculated in QCD perturbation theory, however it has remained a popular jet measure because it can be easily determined.

In order to obtain corrected sphericity distributions we followed the same procedure discussed in the previous section. The fully corrected sphericity distributions for c.m. energies from 7.7 to 31.6 GeV are shown in Fig. 3. The trend observed in the data is very similar to that exhibited by the thrust distributions, namely the sphericity distributions become narrower as the energy increases, while the position of the peak shifts towards low values. These features are well described at all energies by Monte Carlo models including QCD effects [10, 13, 14] while the Field and Feynman model [12] describes the data below 20 GeV

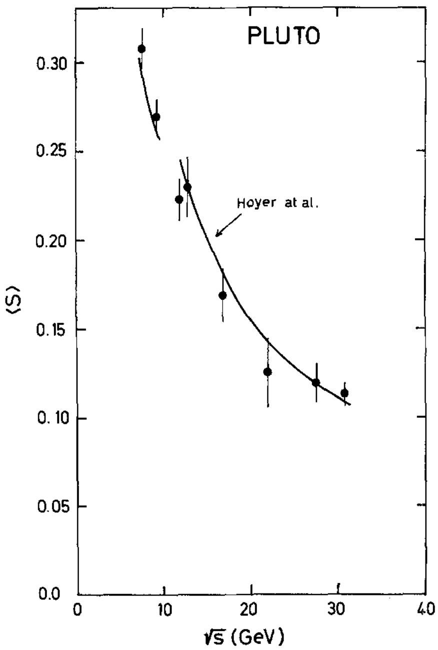

Fig. 4. Mean sphericity values as a function of c.m. energy. The solid curve represents the expectations from the Hoyer et al. Monte Carlo program

but fails to describe the tail in sphericity distribution at higher energies. The mean value $\langle S\rangle$ as a function of c.m. energy is shown in Fig. 4. Here again the trend is similar to that previously discussed for $\langle 1-T\rangle$ namely that there is a steep decrease in $\langle S\rangle$ at low c.m. energies that tends to flatten out above ~ 20 GeV.

V. Opening Angle

The energy weighted jet opening angle, which has the advantage of being calculable in QCD perturbation theory [20] is defined as

$$\langle \sin^2\eta\rangle = \left\langle \frac{E\sin^2\delta}{\sqrt{s}}\right\rangle, \tag{8}$$

where E denotes the energy of a given particle and δ stands for the angle between this particle and the jet axis. This quantity, fully corrected for detector and radiative effects is shown in Fig. 5 as a function of c.m. energy $\sqrt{s}$. It shows the same trend as that observed for $\langle S\rangle$ or $\langle 1-T\rangle$. Also from Fig. 5 it can be seen that a good description of the data can be obtained by the sum of a QCD term and a non-perturbative contribution of the form [20]

$$\langle \sin^2\eta\rangle = \frac{2\alpha_s}{\pi} + \frac{\pi C\langle p_T\rangle_{\mathrm{NP}}}{2\sqrt{s}}, \tag{9}$$

* Unlike thrust the sphericity measured in an ideal detector is not unique. Our corrected values refer to a final state in which neutral pions have already decayed. Treating them as stable particles produces a change of typically $\lesssim 5\%$. Furthermore since sphericity is a quadratic quantitiy it is more sensitive to measurement errors than thrust

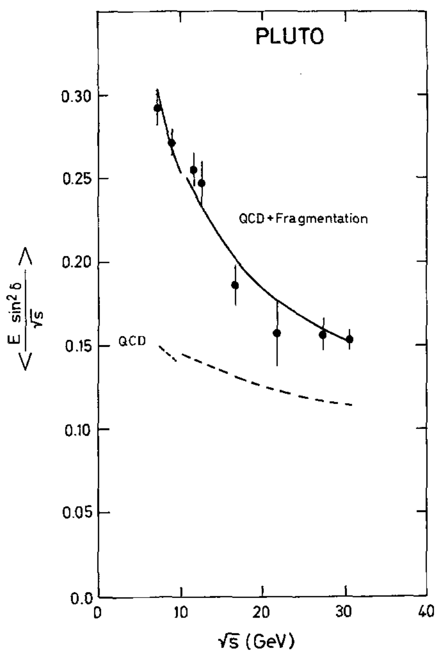

Fig. 5. The mean opening angle of a jet as a function of energy. The solid curve represents the results of fitting the linear sum of a perturbative QCD term (dashed line) and a fragmentation term. See text for more details

where C is a parameter describing $\langle n \rangle$ as $C \ln \sqrt{s}$. The resulting χ^2 is 6.5 for 6 degrees of freedom and the fitted value for α_s at 30 GeV and for $C\langle p_T \rangle_{\rm NP}$ are 0.18 ± 0.02 and 0.76 ± 0.12 in good agreement to those obtained from similar fits to the energy-energy correlation data in the central region [21] and to those obtained in Sect. III.

VI. Jet Mass Distributions

The jet mass M has recently been proposed as another relevant measure having the advantage of reflecting Lorentz invariant characteristics of jets. The QCD predictions for this quantity have been shown to be infrared stable and several calculations in first and second order [22] as well as in the LLA with next to leading corrections included [23] have recently appeared in the literature.

It has also recently been suggested [15, 16] that the series expansion for M_H^2/s converges faster than that for thrust. Here M_H and M_L are the heavy and light jet invariant masses, resulting after partitioning the final state particles into two jets in such a way that the sum of the squared invariant masses is a minimum [16]. It has been pointed out [22] that first order QCD processes contribute exclusively to the heavy jet, while second order processes contribute to both M_H and M_L. Of particular interest is the difference, $\Delta^2 = M_H^2 - M_L^2$, since here second order QCD contributions – and at the level of hadrons also the non-perturbative effects – partly cancel, leaving first order contributions as the dominating effect.

In the experiment, the few original hard partons are not observable, but the jet mass is reconstructed from typically 30 photons and stable charged particles. From a study of simulated $q\bar{q}$ and $q\bar{q}g$ events we found that the prescription of minimizing $M_H^2 + M_L^2$ introduces biases due to the following effects: *i)* There are considerable fluctuations in the fragmentation process increasing systematically the heavy mass. *ii)* Partitioning the observed particles by minimizing $M_H^2 + M_L^2$ has the trend of making M_L^2 and M_H^2 more similar to each other.* This indicates the possibility of a spill-over from the first order α_s contribution in M_H to M_L. Since details of the fragmentation process are unknown, we do not correct for these biases. In view of these systematic uncertainties the fits discussed below have to be interpreted with care.

The correction for measurement errors and acceptance losses of the jet invariant mass is more elaborate than that of the previously discussed measures thrust and sphericity. This is due to our lack of knowledge of charged particle masses and to particle losses. Our Monte Carlo studies show that the jet mass distribution for a generated sample of events is considerably degraded after imposing acceptance cuts and detector effects. Therefore the correction method described in Sect. III cannot be safely applied here. Instead we use a weighting procedure similar to the one employed in the determination of particle multiplicities [18] to correct the observed $M_{H,L}^2/s$ values. In brief we calculate the conditional probability distribution for the generated invariant mass given the measured one using Monte Carlo events before and after passing them through a complete detector simulation.

The jet invariant mass distributions M_H^2/s and M_L^2/s, corrected as discussed above, are presented in Figs. 6 and 7 respectively. The trend shown by both sets of data is similar to that discussed in previous sections for thrust and sphericity distributions, namely as the energy increases the distributions of M_H^2/s and M_L^2/s become narrower and the position of the peak shifts towards smaller values. This is another indication of the stronger two-jet character of high energy annihilation events. The Monte Carlo calculations according to Hoyer et al. [10] (full curve) describe the data very well, in contrast to the perturbative QCD prediction in the LLA [23a]. Since this QCD prediction depends on one parameter, Λ, the

* Similar effects are observed if the thrust axis is used for partitioning the events

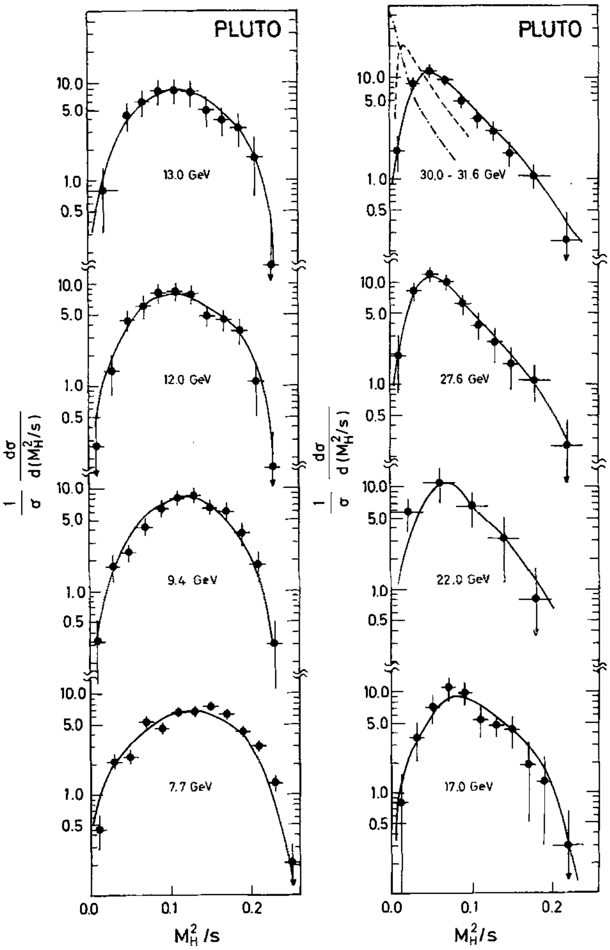

Fig. 6. Normalized heavy jet mass distributions from 7.7 to 31.6 GeV. The solid curves represent the expectations from Hoyer et al. Monte Carlo. For the sake of illustration the dotted line shows the prediction at our highest energy of a leading log calculation for two values of Λ namely 0.2 (dashed-dotted line) and 1.8 GeV (dashed line). Notice that this prediction depends very weakly on c.m. energy

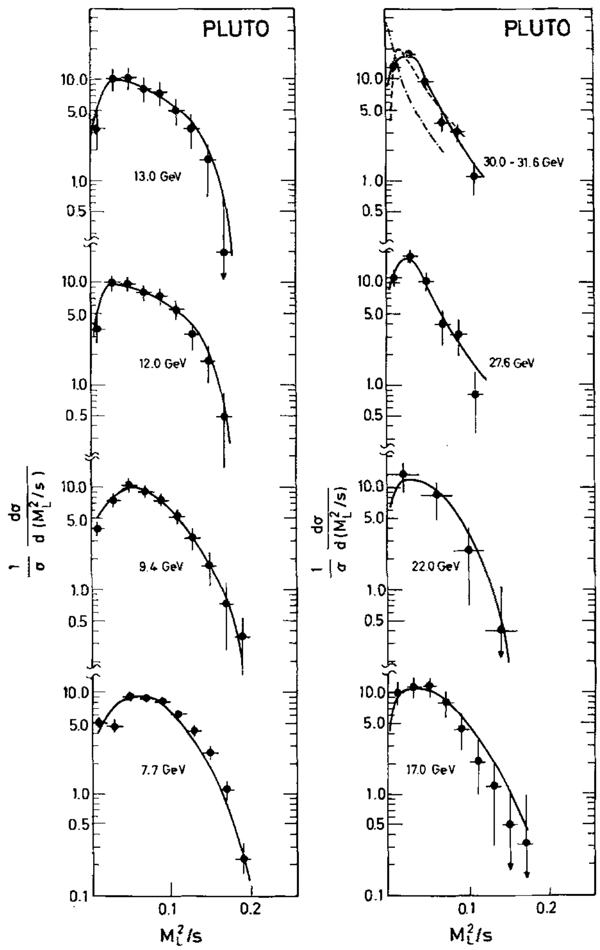

Fig. 7. Normalized light jet mass distributions from 7.7 to 31.6 GeV. The solid curves represent the expectations from Hoyer et al. Monte Carlo. For illustrative purpose the dotted line shows the prediction at our highest energy of a leading log calculation using two values of Λ namely 0.2 GeV (dashed-dotted line) and 1.8 GeV (dashed line)

scale in strong interactions, we show the QCD curves for two given values of Λ, 0.2 and 1.8 GeV. This shows how approximations to QCD can mimic fragmentation effects if a large value of Λ is used. In Fig. 8 we also show acceptance corrected data on $(M_H^2-M_L^2)/s$. Notice that though the $(M_H^2-M_L^2)/s$ distributions shrink with energy they do so very slowly.

In Fig. 9a, b we show the energy dependence of the average values $\langle M_H^2/s\rangle$, $\langle M_L^2/s\rangle$. It reflects again the narrowing of both the heavy and the light jet with energy. However the difference $\langle (M_H^2-M_L^2)/s\rangle$, see Fig. 9c, decreases very little with energy. In analogy to what has been discussed in previous sections we try next to describe the energy dependence of $\langle M_H^2/s\rangle$ as the linear sum of a QCD term and a fragmentation term. To be more specific we fit the experimental data on $\langle M_H^2/s\rangle$ to

$$\left\langle \frac{M_H^2}{s} \right\rangle = 1.05\left(\frac{\alpha_s}{\pi}\right) + \frac{C_H}{\sqrt{s}}, \tag{10}$$

where the first term on the right hand side of (10) represents the perturbative QCD prediction [16] and the last term represents the fragmentation contribution which we simply parametrize as proportional to $1/\sqrt{s}$ following our discussion in Sect. III and considering the first order relation $1-T=M_H^2/s$. The resulting $\chi^2/\mathrm{NDF}=6.7/7$ is good and the best estimates for C_H and α_s are 0.3 ± 0.1 GeV and 0.20 ± 0.02 at 30 GeV, respectively. Taking into account second order corrections, the term $6.9\left(\frac{\alpha_s}{\pi}\right)^2$ has to be added to (10) [16].

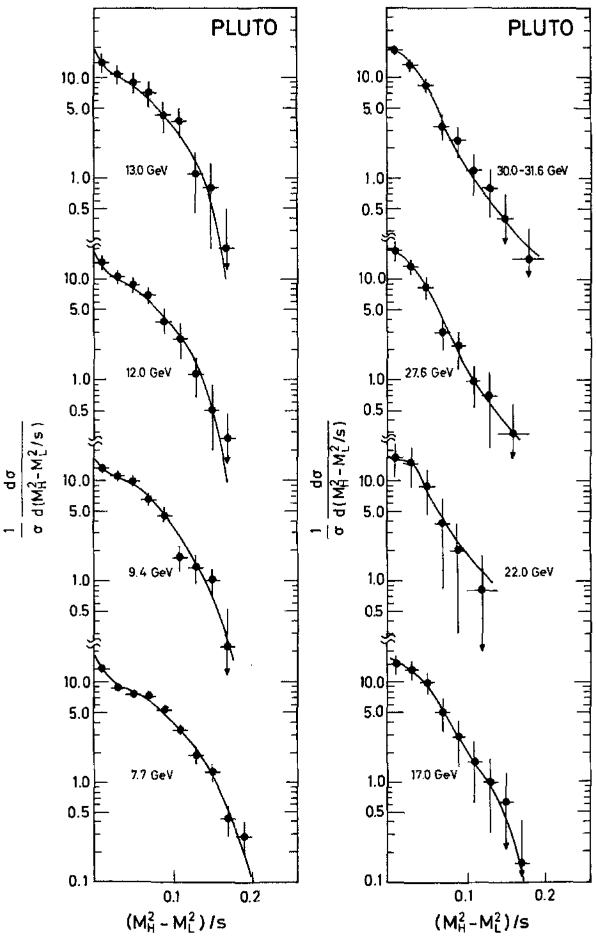

Fig. 8. Normalized distribution of the difference between the squares of the heavy and light jet masses. The solid curve represents the expectations from Hoyer et al. Monte Carlo

As already discussed in the case of thrust this does not change the fit or the non-perturbative part but merely reduces the value of $\alpha_s(\sqrt{s}=30\,\text{GeV})$ to 0.15 ± 0.02 (see footnote* on p. 300).

We finally would like to point out that the energy dependence of $\left\langle\frac{M_H^2-M_L^2}{s}\right\rangle$ is well described by a second order perturbative QCD prediction alone [16] namely

$$\left\langle\frac{M_H^2-M_L^2}{s}\right\rangle=1.05\left(\frac{\alpha_s}{\pi}\right)+2.92\left(\frac{\alpha_s}{\pi}\right)^2 \tag{11}$$

as shown in Fig. 9c. The resulting χ^2/NDF is 10.0/7 and the best estimate for $\alpha_s(\sqrt{s}=30\,\text{GeV})$ is 0.11 ±0.01. The difference between the quoted values for $\alpha_s(\sqrt{s}=30\,\text{GeV})$ obtained from various first or second order expressions, which is roughly 0.04, can be considered as an estimate not only of our experimental

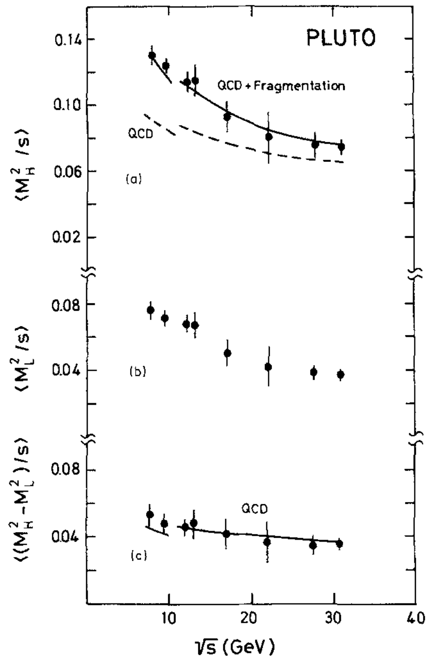

Fig. 9a–c. The dependence on c.m. energy of the mean squared heavy jet mass, the mean squared light jet mass and of the mean of their difference. The solid curve in **a** represents the results of a fit to the linear sum of a perturbative term (dotted line) and a phenomenological fragmentation term. The solid curve in **c** shows the results of a fit to a second order QCD prediction with no fragmentation

systematic errors but also of the uncertainties introduced by our ansatz about the behaviour of the non-perturbative contributions.

VII. Multiplicity and Event Topology

An important observable which characterizes hadronic states is the particle multiplicity. Earlier measurements [24] have shown a slow logarithmic rise

$$\langle n_{ch}\rangle=2.1+0.85\ln s \tag{12}$$

at low energies, and an almost three times stronger rise (with $\ln s$) above 10 GeV [18, 25]. Starting at about this energy jets also become wider than expected from the Field-Feynman description, as visible in p_T^2 [2] and in the jet measures described above.

This coincidence suggests that both phenomena are correlated, and that the rapid rise occurs predominantly in wide jets. On the other hand, the rapid multiplicity rise may just be a purely kinematic effect in the 2-jet topology and may be common to both narrower and wider jets. This alternative would also be suggested by LLA calculations of the jet evolution [26], which connect the multiplicity with those of the partons at the end of the cascade. That number would be largely independent of whether the first emitted gluon had induced a wide or a narrow topology [27].

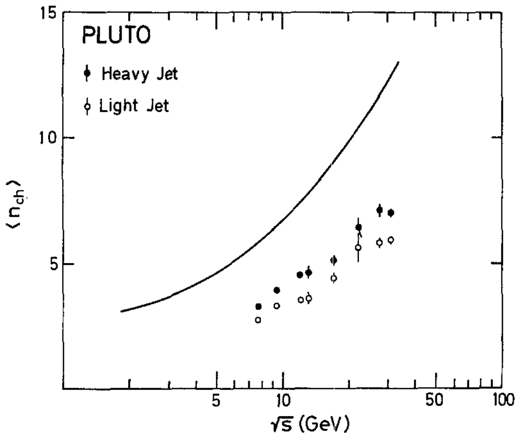

Fig. 10. Mean charge multiplicity of the heavy and light jets as a function of c.m. energy. The solid curve describes the energy dependence of the event mean charge multiplicity

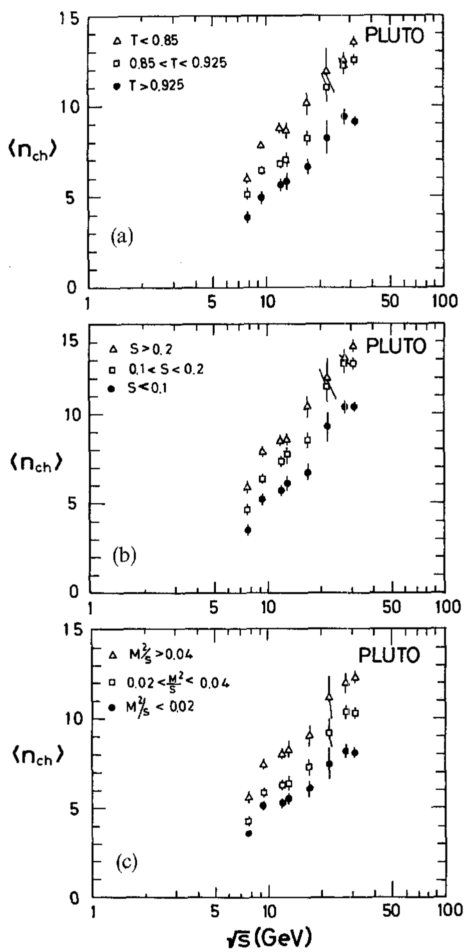

Fig. 11a–c. Mean charged multiplicity as a function of c.m. energy for three different slices in thrust, sphericity and jet invariant mass

In order to distinguish between these two extreme possibilities, we have evaluated the mean charged multiplicity (corrected for detector effects and initial state radiation) for several classes of different jet widths. Figure 10 shows the energy dependence of the multiplicity separately for the heavy (=wide) and light (=narrow) jets as defined in Sect. VI. The average multiplicity of the heavy jets is larger, as trivially expected from the constant $-p_T$ fragmentation process. The relative rise $\frac{1}{\langle n\rangle}\frac{d\langle n\rangle}{ds}$, however, is the same for heavy and light jets, and excludes the hypothesis that the hard gluon radiation observed at PETRA energies is the dominant source of the multiplicity rise.

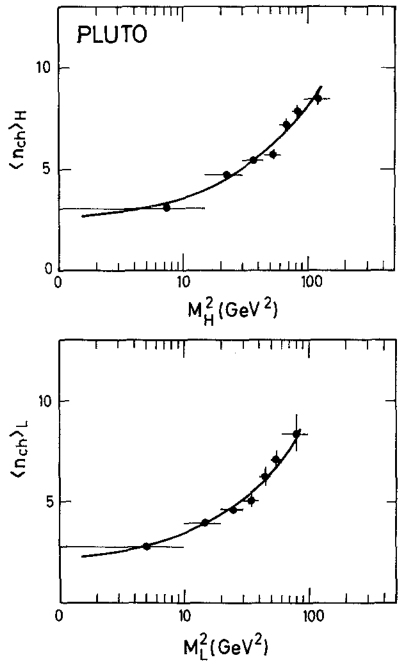

Fig. 12. Mean charge multiplicity of the heavy and light jets as a function of their squared masses for the 27.6–31.6 GeV sample. The solid curves show the results of fitting the LLA equation (13)

Figure 11a–c show the multiplicities for other classes of different jet widths, as defined by cuts in thrust (11a), sphericity (11b) and in the jet masses (11c), with again a similar relative rise of the multiplicity for all classes, and the same conclusions against the hard gluon radiation as the dominant source. This conclusion agrees with the results of the current Monte Carlo calculations which attribute only a small multiplicity increase (≈ 0 at 10 GeV and ≈ 1 unit at 30 GeV) to the hard gluon [28].

The evaluation of the jet masses as described in Sect. VI allows, in addition, a special test of the LLA theory of the jet evolution [26]. It has been shown before [18] that all multiplicity data in the range $5 \leq s \leq 1000\,\mathrm{GeV}^2$ can be reasonably well described by

$$\langle n_{\mathrm{ch}}\rangle = a + b\exp(c\sqrt{\ln Q^2/\Lambda^2}) \tag{13}$$

with Q^2 set to the invariant mass of the two-jet system, $Q^2 = s$ (typical fit values are $a = 2.38 \pm 0.09$, $b = 0.04 \pm 0.01$, with $c = 2.4$ and $\Lambda = 500$ MeV fixed). It has also been suggested to apply (13) to the multiplicity of single jets [29]. Then the virtual mass of the parent parton, $Q^2 = M_{\mathrm{JET}}^2$ has to be inserted into the formula (13). This is shown in Fig. 12, which gives the multiplicity of single jets as a function of the jet mass, separately for the light and heavy one, with the solid curves representing the fit to the formula (13). With the fixed parameters $c=2.4$ and $\Lambda=500$ MeV, one obtains fit parameters $a=0.91\pm0.19$ (0.62 ± 0.19) and $b=0.019\pm0.001$ (0.021 ± 0.001) for the heavy (light) jets. It is interesting to note that both the parameters describing the multiplicity for the light and heavy jets agree within errors and result in a dependence of $\langle n_{\mathrm{ch}}\rangle_{\mathrm{jet}}$ as a function of jet mass which is very similar to the c.m. energy dependence of the event mean charged multiplicity.

VIII. Summary and Conclusions

The differential distributions of thrust, sphericity, and of jet masses have been measured over the energy range $7.7 \leqq s \leqq 31.6$ GeV. This data, fully corrected for detector and radiative effects, can be well described at all energies by existing Monte Carlo calculations, including QCD effects [10, 13, 14]. The Field and Feynman model [12] describes the data only at low energies.

None of the QCD predictions available describe the data. However $\langle 1-T\rangle$, $\langle \sin^2\eta\rangle$ and $\langle M_H^2/s\rangle$ can be well described by the sum of a QCD term and a simple ansatz for the fragmentation contribution. This indicates that at 30 GeV on the average 60% of the jet spread can be calculated in QCD and still $\sim 40\%$ is due to confinement effects. At LEP energies of about 100 GeV non-perturbative effects will be reduced to a level of about 10%.

The values of α_s obtained from the fits to various jet measures are consistent among each other, and reasonably close to the results of more dedicated determinations, thus confirming the simple ansatz of a $1/\sqrt{s}$ decrease of the non-perturbative effects.

The mean charged multiplicity $\langle n_{\mathrm{ch}}\rangle$ has been measured as a function of c.m. energy and different jet measures. As expected $\langle n_{\mathrm{ch}}\rangle$ is larger for heavier jets, however, the increase with energy is similar for both the light and the heavy jet thus excluding the hypothesis that hard gluon radiation is the dominant source of the steep multiplicity increase observed at PETRA. The dependence of $\langle n_{\mathrm{ch}}\rangle_{\mathrm{jet}}$ on its mass is consistent with LLA calculations.

Acknowledgements. We wish to thank the members of the DESY Directorate for the hospitality extended to the University groups. We thank Prof. Clavelli for a helpful discussion. We are indebted to the PETRA machine group and the DESY computer center for their excellent performance during the experiment. We gratefully acknowledge the efforts of all engineers and technicians of the collaborating institutions who have participated in the construction and the maintenance of the apparatus.

References

1. a) G.Hanson et al.: Phys. Rev. Lett. **35**, 1609 (1975)
   b) PLUTO Collaboration Ch.Berger et al.: Phys. Lett. **78** B, 176 (1978)
2. a) JADE Collaboration W.Bartel et al.: Phys. Lett. **91** B, 142 (1980)
   b) MARK J Collaboration D.P.Barber et al.: Phys. Rev. Lett. **43**, 830 (1979)
   c) PLUTO Collaboration Ch.Berger et al.: Phys. Lett. **86** B, 418 (1979)
   d) TASSO Collaboration R.Brandelik et al.: Phys. Lett. **86** B, 243 (1979)
3. a) TASSO Collaboration R.Brandelik et al.: Phys. Lett. **97** B, 453 (1980)
   b) TASSO Collaboration R.Brandelik et al.: Phys. Lett. **94** B, 437 (1980)
   c) MARK J Collaboration D.P.Barber et al.: Phys. Lett. **89** B, 139 (1979)
   d) TASSO Collaboration R.Brandelik et al.: Z. Phys. C – Particles and Fields **4**, 87 (1980)
4. PLUTO Collaboration Ch.Berger et al.: Phys. Lett. **97** B, 459 (1980)
5. A. de Rújula et al.: Nucl. Phys. B **138**, 387 (1978)
6. PLUTO Collaboration Ch.Berger et al.: Z. Phys. C – Particles and Fields **4**, 269 (1980)
7. PLUTO Collaboration Ch.Berger et al.: Phys. Lett. **90** B, 312 (1980); **91** B, 148 (1980)
8. O.Achterberg: Thesis, Hamburg, Univ. (1981)
9. S.Brandt, Ch.Peyrou, R.Sosnowski, A.Wroblewski: Phys. Lett. **12**, 57 (1964)
   E.Farhi: Phys. Rev. Lett. **39**, 1587 (1977)
10. P.Hoyer et al.: Nucl. Phys. B **161**, 349 (1979)
11. J.B.Babcock, R.E.Cutkovsky: Nucl. Phys. B **176**, 113 (1980)
12. R.D.Field, R.P.Feynman: Phys. Rev. D **15**, 2590 (1977); Nucl. Phys. B **136**, 1 (1978)
13. A.Ali et al.: Phys. Lett. **82** B, 285 (1979); Nucl. Phys. B **167**, 454 (1980)
14. a) P.Mazzanti, R.Odorico: Phys. Lett. **95** B, 133 (1980)
    b) G.Fox, S.Wolfram: Nucl. Phys. B **168**, 285 (1980)
15. R.K.Ellis, D.A.Ross, A.E.Terrano: Phys. Rev. Lett. **45**, 1226 (1980); Nucl. Phys. B **178**, 421 (1981)
16. L.Clavelli, D.Wyler: Phys. Lett. **103** B, 383 (1981)
17. G.Schierholz: DESY 1979/71
18. PLUTO Collaboration Ch.Berger et al.: Phys. Lett. **95** B, 313 (1980)
19. J.D.Bjorken, S.J.Brodsky: Phys. Rev. D **1**, 1416 (1970)
20. C.L.Basham, L.S.Brown, S.D.Ellis, S.T.Love: Phys. Rev. D **17**, 2298 (1978)
21. PLUTO Collaboration Ch.Berger et al.: Phys. Lett. **99** B, 292 (1981)
22. a) L.Clavelli: Phys. Lett. **85** B, 111 (1979)
    b) T.Chandramohan, L.Clavelli: Phys. Lett. **94** B, 409 (1980)
23. a) A.V.Smilga: Nucl. Phys. B **161**, 449 (1979)
    b) F.Gutbrod: DESY 1980/06
24. C.Bacci et al.: Phys. Lett. **86** B, 234 (1979)
    J.L.Siegrist: Ph.D. Thesis, SLAC 225-UC 34d (1980)
25. TASSO Collaboration R.Brandelik et al.: Phys. Lett. **89** B, 418 (1980)
    JADE Collaboration W.Bartel et al.: Phys. Lett. **88** B, 171 (1979)
26. a) W.Furmanski, S.Pokorski: Nucl. Phys. **155** B, 253 (1979)
    b) A.Bassetto, M.Ciafaloni, G.Marchesini: Phys. Lett. **83** B, 207 (1979)
27. G.Parisi: Private communication
28. G.Wolf: DESY 80/85
    L.Criegee, G.Knies: DESY 81/044 (submitted to Phys. Rep.)
29. W.Furmanski, R.Petronzio: Private communication